Nonlinear response and failure mechanism of infilled RC frame structures under biaxial seismic excitation

Y. P. YUEN and J. S. KUANG
The Hong Kong University of Science and Technology, Hong Kong China

SUMMARY:
Masonry-infilled reinforce concrete frame structures are very common structural forms for buildings. In practice, infill walls are usually treated as non-structural components and their influence to overall structure is very often ignored. Even if their structural effect on the building is considered, the in-plane and out-of-plane behaviours of infilled RC frames are treated and analysed separately. This study aims to investigate the behaviour of infilled RC-frame structures under uniaxial and biaxial seismic excitations. Nonlinear response history analyses for three types of frame structure, namely bare frames, fully infilled frames and 2/3-storey-height infilled frames, under realistic earthquakes are performed. The simulations successfully replicated the expected hysteresis behaviour and damage patterns of the prototype RC infilled frames under earthquakes. Based on the analysis results, it is found that the structural behaviour of infilled frame structures under biaxial or uniaxial seismic excitations can be very different. Fully integrated infill-wall panels can enhance the stability and energy dissipation of the structures. However, out-of-plane collapse of infills under biaxial excitation would spoil the force transfer mechanisms and vertical supporting action that seriously jeopardise the structure stability. It is also observed that the design concept of “strong column-weak beam” may not be applied to the infilled frames since the structural behaviour of the frames is altered by the infills.

Keywords: infilled frame, biaxial excitation, discrete finite element, out-of-plane

1. INTRODUCTION

Infilled reinforce concrete (RC) frame structures are recognised as one of the most common structural forms for low- to medium-rise buildings in the world. In conventional design practice, infill walls of a building frame are normally considered as non-structural members, hence their influence to the overall performance of the structure is ignored. Reports on the failure of infilled RC frame structures during devastating earthquakes have revealed that ignoring the infill effect on the structure behaviour may jeopardise the earthquake-resistant ability of the building. Recently, some modelling or design methods of infilled frame structures have been implemented in some modern design codes such as ASCE41. It is specified that when an infilled frame is subjected to both in-plane and out-of-plane loads, it will be analysed separately in the orthogonal directions. However, the interacting in-plane and out-of-plane structural action can significantly affect the performance of the infilled frame, and a reduction of as most as 50% in the static lateral load carrying capacity due to influence of out-of-plane has been reported in the literature (Flanagan and Bennett, 1999; Hashemi and Mosalam, 2007; Kuang and Yuen, 2010). Thus, the actual infill-frame interaction so as the seismic behaviour of the structure may not be captured from the analysis if the combining effect is neglected. This study aims to investigate the behaviour of infilled RC frame structures under uniaxial and biaxial seismic excitations while the focus is on the local infill-frame interaction. Two types of masonry-infill configuration in frames are considered: full infills and 2/3-storey-height infills Nonlinear response history analyses of infilled RC frames under four earthquakes, namely, 1979 El-Centro, 1987 Superstition-Hill, 1995 Kobe and 1999 Chi-Chi earthquakes, are conducted using discrete finite-element analysis with damage-based material models.

2. INFILLED RC FRAME STRUCTURE MODELS

2.1 RC Frame Structure

The prototype structure adopted is based on a 2-storey RC building frame shown in **Figure 2.1**, which was designed to resist earthquakes with PGA of 0.15g and detailed to obtain an expected displacement ductility factor between 2 to 4. The frame structure is infilled with masonry walls along the NS direction while no infills are deployed along the EW direction. Two different types of infill configuration: full infills and 2/3-storey-height infills are considered. The infill panels are composed of 600 × 300 × 125-mm masonry units and 10-mm thick mortar joints.

2.2 Modelling and Analysis Techniques

To adequately capture the local infill-frame interacting behaviour, detailed modelling and discretization of the frame and infill components are inevitable which require high computational effort. Yet, it is possible to reduce the computation cost and able to obtain the interested local behaviour by utilising sub-modelling approach. It is noticed that the building is more vulnerable to earthquakes along the NS direction comparing with the EW direction. Furthermore, due to having low out-of-plane stiffness the infilles have little effect on the seismic responses of the frame along the EW direction. Therefore, the simplified global frame model can be firstly used to study the responses of the building incurred the EW seismic excitation and the obtained response displacement

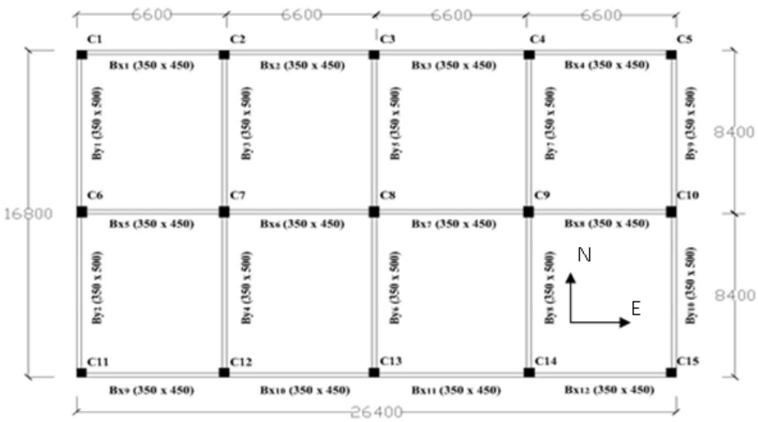

(a) Floor plan outline

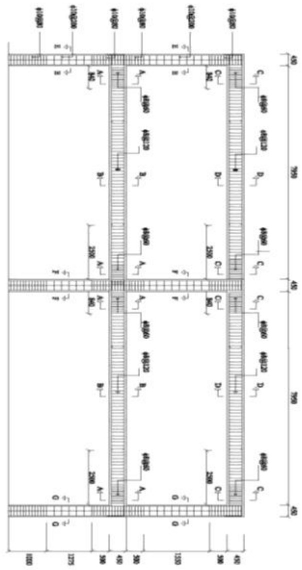

(b) Frame NS

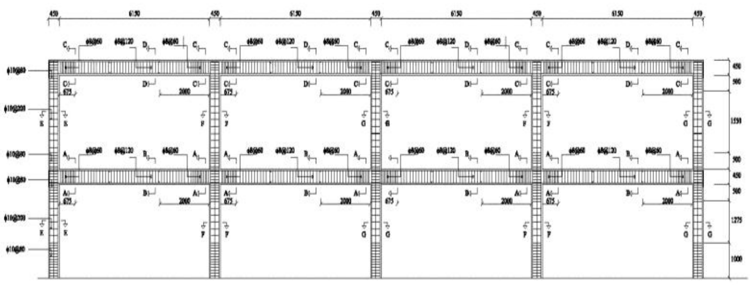

(c) Frame EW

Figure 2.1. Dimensions and reinforcement details of prototype RC structure (mm)

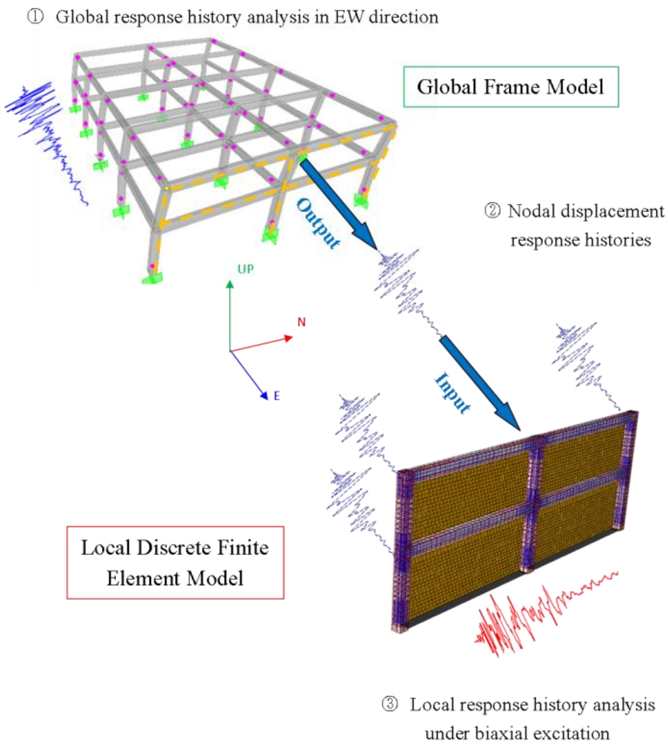

Figure 2.2 Schematic diagram of modelling and analysis procedure

histories of different joints in the global model are then input to the corresponding nodes of the detailed local model of the frame NS as shown in **Figure 2.1,** while the NS seismic excitation is applied simultaneously to achieve a biaxial excitation analysis. **Figure 2.2** shows the schematic diagram of the modelling and analysis procedures.

The global finite element model for the whole building frame is constructed by following the standard approach using SAP2000 (CSI, 2010), where plastic hinges are assigned to the frame member ends. The detailed local model is constructed with ABAQUS, while all components are discretely modelled with appropriate elements and mechanical interactions are enforced amongst them. The concrete frame and masonry units are discretised into linear 8-node, 3-D solid elements and their mechanical behaviour is modelled with the smeared isotropic damage-plasticity law (Lubliner et al., 1989). The embedded steel reinforcement is modelled with 2-node, 3-D truss element and modified Menegotto-Pinto model (Sakai and Kawashima, 2003) is used to present the constitutive relationship. As the strength of mortar joints is often much weaker than that of masonry units in infill walls, damage and cracks would very likely propagate along the joints. To simulate the pre- and post-fracture behaviour of mortar joints, the damage-based cohesive interactions with finite sliding formulation are enforced on the contact surfaces of the masonry units (Yuen and Kuang, 2011). The traction-separation law for cohesive surface considering the mixed-mode fracture behaviour of the mortar joints is

$$\mathbf{t} = (1-D)\mathbf{k}_e[\mathbf{u}] \tag{2.1}$$

where $\mathbf{t}$ and $[\mathbf{u}]$ are the traction and displacement jump vector between two masonry unit surfaces respectively; $\mathbf{k_e}$ is an initial isotropic elastic stiffness tensor; and D is a scalar damage parameter of value within [0,1]. The criterion of damage initiation is defined as

$$t_n^2 + \beta_s^2 t_s^2 + \beta_t^2 t_t^2 - f_{nt}^2 = 0 \qquad (t_n \geq 0) \tag{2.2}$$

$$\beta_s^2(|t_s| + t_n \tan\phi_s)^2 + \beta_t^2(|t_t| + t_n \tan\phi_t)^2 - f_{nt}^2 = 0 \qquad (t_n < 0) \tag{2.3}$$

where f_{nt} is tensile strength of the mortar joints; β_s and β_t are the ratios of the mode II shear cohesion strength c_s and mode III tear cohesion strength c_t to the tensile strength respectively; ϕ_s and ϕ_t are the friction angles under mode II and mode III deformation respectively. It is assumed that critical strain-energy release rate G_c under mixed-mode fracture is represented by (Benzeggagh and Kenane, 1996)

$$G_C = G_C^I + (G_C^{II} + G_C^{III} - G_C^I)\left(\frac{G_C^{II} + G_C^{III}}{G_T}\right)^m \tag{2.4}$$

and the evolution of damage is assumed with the following form

$$D = \frac{G_T([\mathbf{u}]) - G_0}{G_C - G_0} \tag{2.5}$$

where G_T is the total strain energy release rate; $G^I{}_C$, $G^{II}{}_C$, and $G^{III}{}_C$ are critical strain-energy release rate under pure mode I pure model II and mode III fracture respectively; m is an exponent depends on the brittleness of the material; G_0 is strain-energy release rate at damage initiation.

The interfacial interaction between the frame and infills is modelled as a frictional contact problem enforced with penalty method, where the contacting surfaces are assumed as cohesionless. The maximum meshing size for the frame and steel bars is not greater than 200 mm and the mesh is refined to 80 mm at the stress concentration zones, while for the infills the meshing size is approximately 150 mm. On the other hand, several reaction mass-springs aligned with the EW axis are attached to the corners in the local model, of which elasto-plastic and inertia properties are calibrated to obtain an equivalent dynamic behaviour of the local model to the global model along the EW axis.

Due to the highly nonlinear nature of the simulation problem that involves nonlinear material responses, complicated and evolving constraints and contacts among components and nonlinear geometric effects, the response history analysis employs an explicit central-difference integration scheme with time increment of 1^{-7}s, while double-precision numbers are used in the analysis to retain sufficient precision.

2.3 Characteristics of Natural Vibration Modes

The first three natural vibration modes of the global and local bare and infilled frame models are extracted, as shown in **Figure 2.3**. Both of the global and local bare frame models have similar modal periods, masses and configurations: the first mode of lateral deflection in NS axis, the second mode of lateral deflection in EW axis and the third mode of twisting, and thus consistent dynamic behaviour of the two models under seismic excitations can be asserted.

The modal characteristics of the two infilled structures are also studied. Due to the strong bracing action provided by the infills to the bare frames, the natural vibration periods of the first lateral deflection modes in the NS axis T_i are significantly reduced from 0.426s to 0.181s for the full infilled frame and to 0.88s for the 2/3-storey-height infilled frame respectively. The effect of infills on the out-of-plane deflection modes, lateral deflection modes in the EW axis and twisting mode are insignificant, and changes in the corresponding vibration periods T_o and T_t are less than 10%.

Furthermore, it is found that total lumped masses on the first and second floors of the local bare frame are 215.76 tons and 191.3 tons respectively. The masonry infills introduced additional masses of 5.45 tons and 3.63 tons to the infilled frames with full infills and 2/3-storey-height infills respectively.

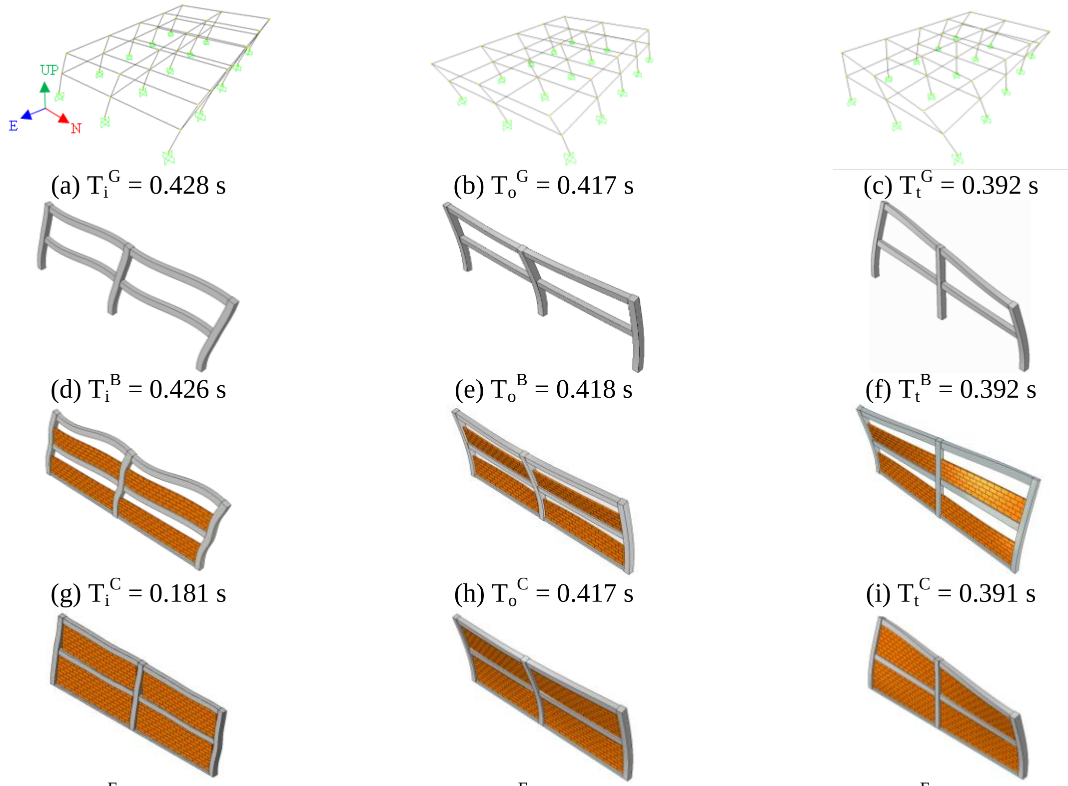

(a) $T_i^G = 0.428$ s (b) $T_o^G = 0.417$ s (c) $T_t^G = 0.392$ s

(d) $T_i^B = 0.426$ s (e) $T_o^B = 0.418$ s (f) $T_t^B = 0.392$ s

(g) $T_i^C = 0.181$ s (h) $T_o^C = 0.417$ s (i) $T_t^C = 0.391$ s

(j) $T_i^F = 0.088$ s (k) $T_o^F = 0.409$ s (l) $T_t^F = 0.388$ s

Figure 2.3. Natural vibration modes of the global and local frames (mass-springs are hidden for simplicity)

3. GROUND MOTION CHRACTERISTICS

Nonlinear response history analysis of the infilled frame structures under biaxial excitations are performed with four realistic earthquakes. The earthquake records adopted in this analysis are 1979 El-Centro at USGS-station 5056 (PGA = 0.14g), 1987 Superstition-Hill at USGS-station 505 (PGA = 0.45g), 1995 Kobe at station Takatori (PGA = 0.65g) and 1999 Chi-Chi (PGA = 0.82g) at station CHY080. The 1979 El-Centro and the 1999 Chi-Chi ground motions can be considered as fortification and rare earthquakes with 475-year and 2436-year return periods respectively, which would be experienced by the prototype RC frame structure. The ground acceleration time histories of the four earthquakes are shown in **Figure 3.1**.

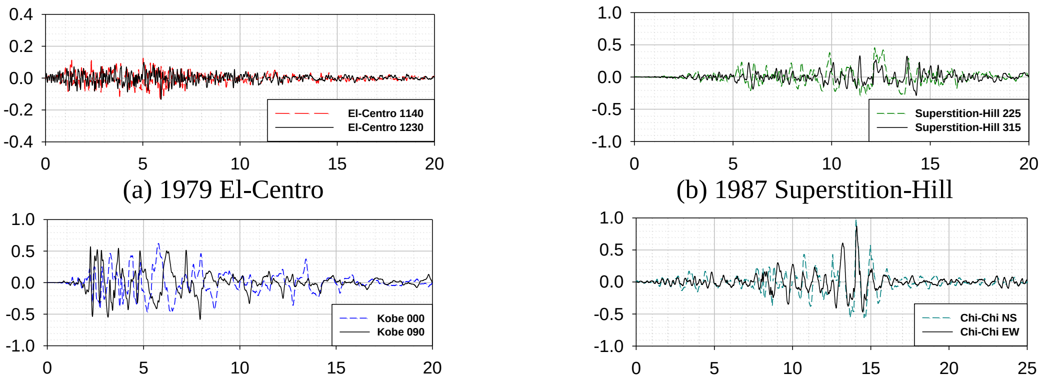

(a) 1979 El-Centro (b) 1987 Superstition-Hill

(c) 1995 Kobe (d) 1999 Chi-Chi

Figure 3.1. Ground acceleration time histories of the four ground-motions
(vertical axis: ground acceleration (g); horizontal axis: time (s))

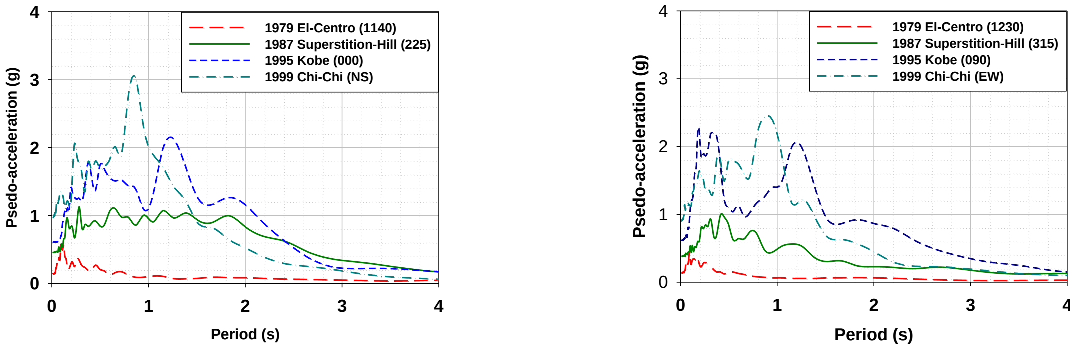

(a) Inputs in NS direction (b) Inputs in EW direction

Figure 3.2. Elastic response spectra of ground-motion histories

The frequency content of the four ground motions are characterised by the elastic response spectra, as shown in **Figure 3.2**, and the mean period $\mathbf{T_m}$ of the corresponding Fourier spectra. The mean periods (s) of the NS and EW components of the earthquakes El-Centro, Superstition-Hill, Kobe and Chi-Chi are (0.49, 0.41), (1.19, 0.71), (1.14, 0.99) and (0.83, 0.87) respectively. Moreover, the Chi-Chi motion is recorded near the source thus its history of ground velocity reveals pulse behaviour.

4. SEISMIC PERFORMANCE OF INFILLED FRAME STRUCTURES

4.1 Analysis Results

Subjected to the four ground motions, the resulted in-plane hysteresis loops, showing base-shear against top drift in the NS direction, of the prototype bare frame and the two infilled RC frame structures are plotted in **Figure 4.1**. The solid-line plots represent the responses of the structures under biaxial excitation, while the dashed-line plots correspond to uniaxial excitation.

The frames behave elastically with minor tensile cracks development on infill panels and frames near corners under the El-Centro earthquake. However, at stronger excitation levels of Superstition-Hill, Kobe and Chi-Chi earthquakes, significant damage and inelastic strain development such as propagation of major cracks running across the whole infill panels and cracking and even crushing of concrete take place in the structures. The incurred deformation shapes and damage distributions on the structures are found to be quite similar under the three strong ground motions and, as an example, contour-plots of the developed equivalent plastic-strain on the structures under the Chi-Chi earthquake are demonstrated in **Figure 4.2**.

4.2 Behaviour of the frames under uniaxial excitations

The bare frame has the stable hysteresis behaviour, as shown in **Figure 4.1**, as typical ductile RC frames do, owing to the successful development of the beam-sway mechanisms that plastic-hinges are formed at the beam ends and column bases as shown in **Figure 4.2**. But the infilled frame structures exhibit different degrees of pinching phenomenon in the hysteresis loops leading to considerable strength and stiffness degradation. The pinching effect is resulted in the cracking of the brittle infills and localised damage in the RC frames. From **Figure 4.2**, it is seen that for the frame with 2/3-storey-height infills, damage is highly localised in the central column at the first storey, and even total failure, i.e. crushing of concrete and buckling of longitudinal reinforcement across the whole column section, occurs therein under the Kobe and Chi-Chi excitations. This is because the central column is restrained on both sides by infills and edge columns are only restrained on one side, thus the central column attracts lateral seismic force that is 1.7~2.6 times higher than that attracted by edge columns. For the fully infilled frame, formation of some plastic hinges in the beams is suppressed by the deformation restraint imposed by the infill panels, but on the contrast the first-storey columns suffer significant shear damage due to the strong thrust caused by the infills' bracing. Furthermore, it is seen that, while plastic hinges cannot be formed in some of the beam ends, some occur in unexpected locations, for instant near the middle of the top beams, in the frame that is also resulted in the bracing action provided by the infills. Since the frame is designed as a typical ductile frame and only the member ends are confined with stirrups, formation of plastic hinges at those unconfined regions would impair the ductility of the structure. It is noticed the global stability of the structures is enhanced by the introduction of fully integrated infills; however, it is demonstrated in the latter section that this stability takes place only if the infill panels do not collapse.

On the other hand, as aforementioned, the initial fundamental frequency of a frame structure can be significantly amplified by infill walls. As a result, the infilled frame structures experience much greater seismic demand than the bare frame; hence the incurred maximum base shears of the infilled frames 2/3-storey-height infills and full infills are 1.5~2.6 and 2.8~5.3 times higher than that of the bare frame. Obviously, the addition strength introduced by the brittle infills is hardly to compensate the elevated forces and thus severer damage is inflicted on the frame members.

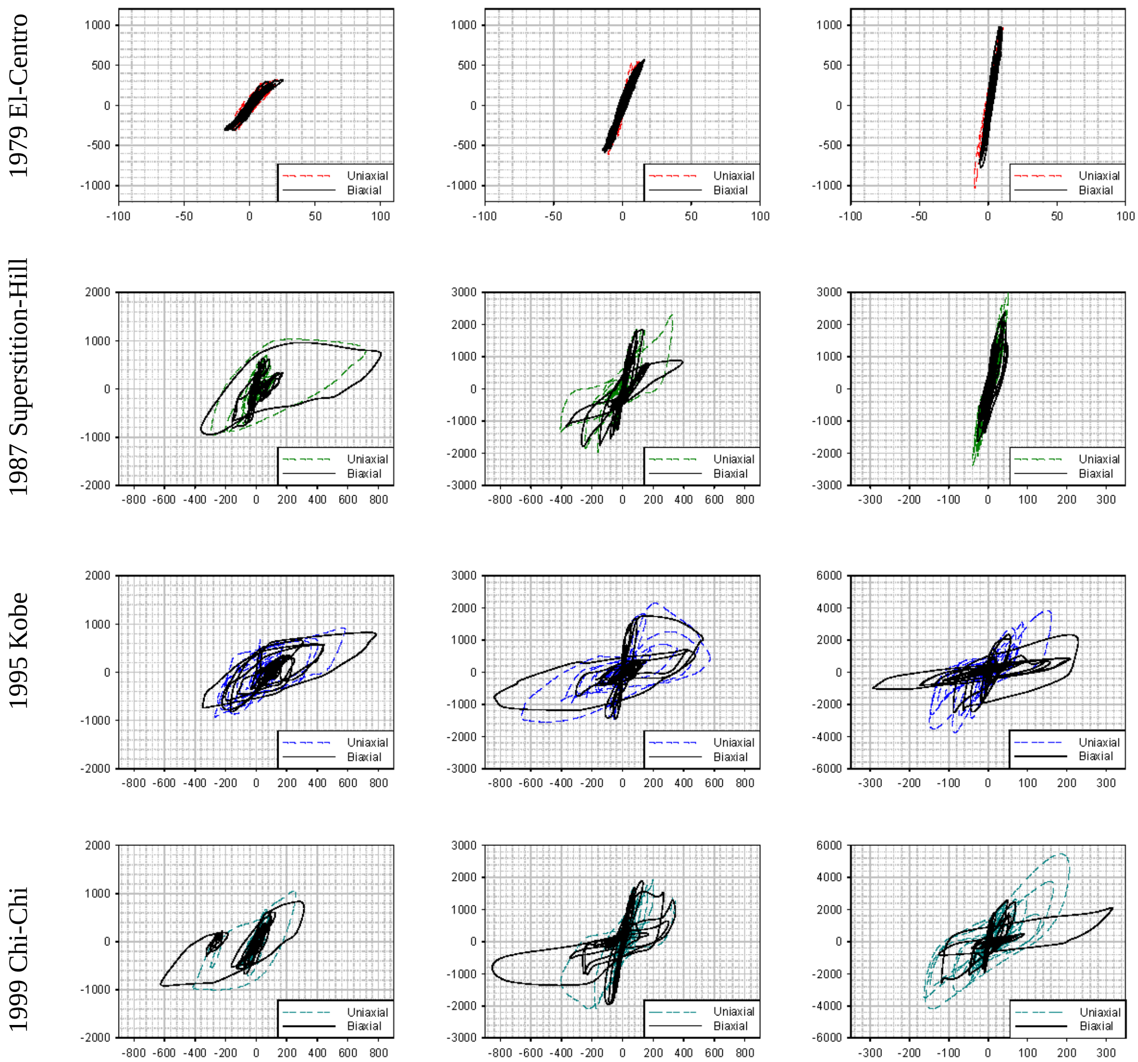

(a) Bare frame (b) 2/3-storey-height infills (c) Full infills

Figure 4.1. In-plane (NS-direction) hysteresis loops of infilled RC frames under four ground-motion histories (vertical axis: base shear (kN); horizontal axis: top drift (mm))

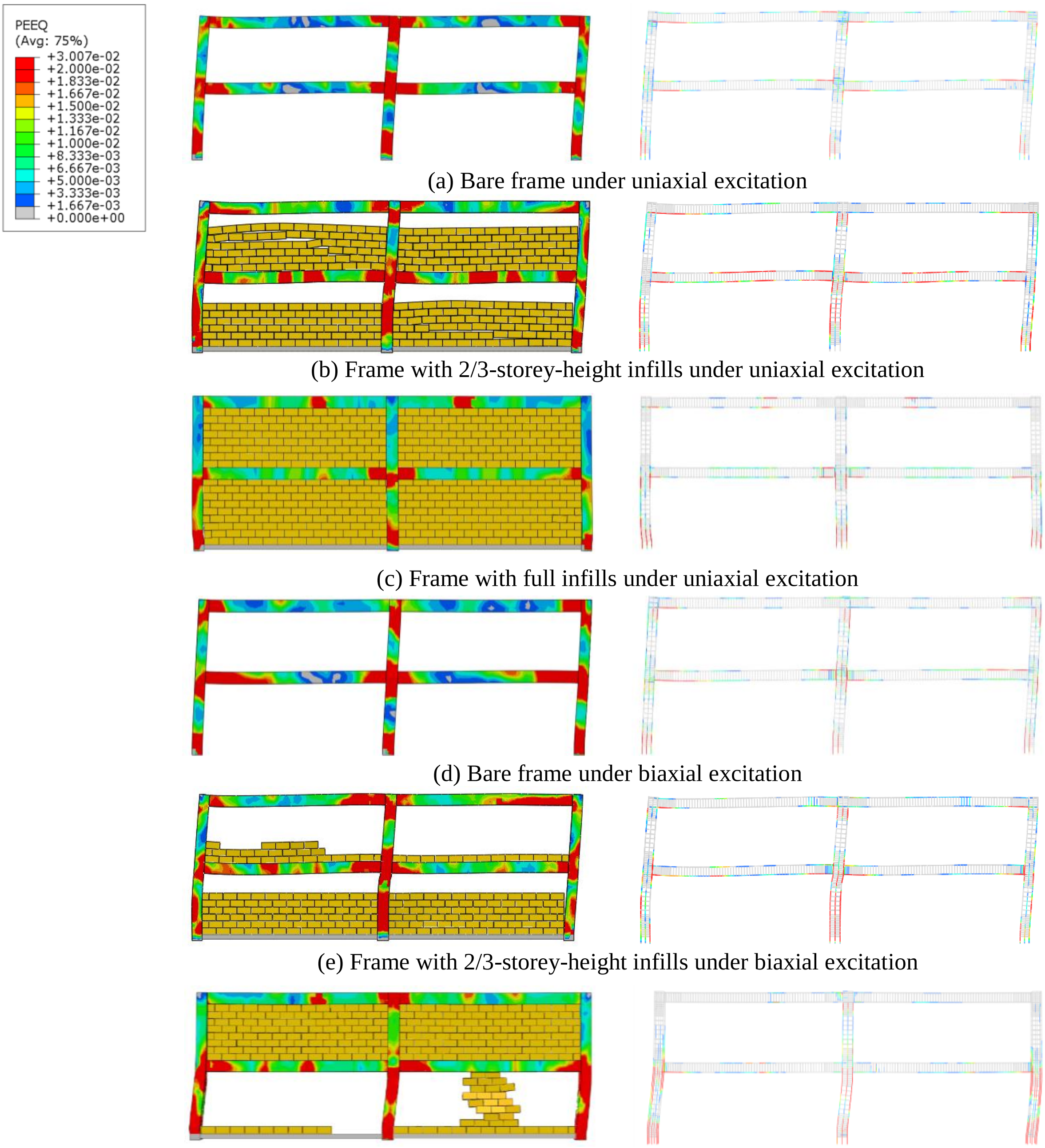

(a) Bare frame under uniaxial excitation

(b) Frame with 2/3-storey-height infills under uniaxial excitation

(c) Frame with full infills under uniaxial excitation

(d) Bare frame under biaxial excitation

(e) Frame with 2/3-storey-height infills under biaxial excitation

(f) Frame with full infills under biaxial excitation

Figure 4.2. Damage pattern of the infilled RC frame structures (t = 14.1 s) under 1999 Chi-Chi earthquake (contour-plot of equivalent plastic-strain)

4.3 Behaviour of the frames under biaxial excitations

When the bare frame structure is subjected to biaxial excitation along both NS and ES directions, as shown in **Figure 4.1**, the global hysteresis behaviour do not deviate too much from the stable hysteresis loops exhibited by the frame under solely uniaxial excitation. The similarity is due to the fact that, as seen in **Figure 4.2**, the inflicted damage mode and regions, where are well confined by stirrups, are quite similar to the case of uniaxial excitation, although addition damage is incurred on the bare frame by the combining two planes seismic loading and that brings on some more pinching effect to the hysteresis loops, in particular for the Chi-Chi case.

Under low intensity of seismic loading, i.e. the El-Centro earthquakes, similar behaviour of the infilled frames under biaxial excitation to that under uniaxial excitation is observed and that indicates that, as

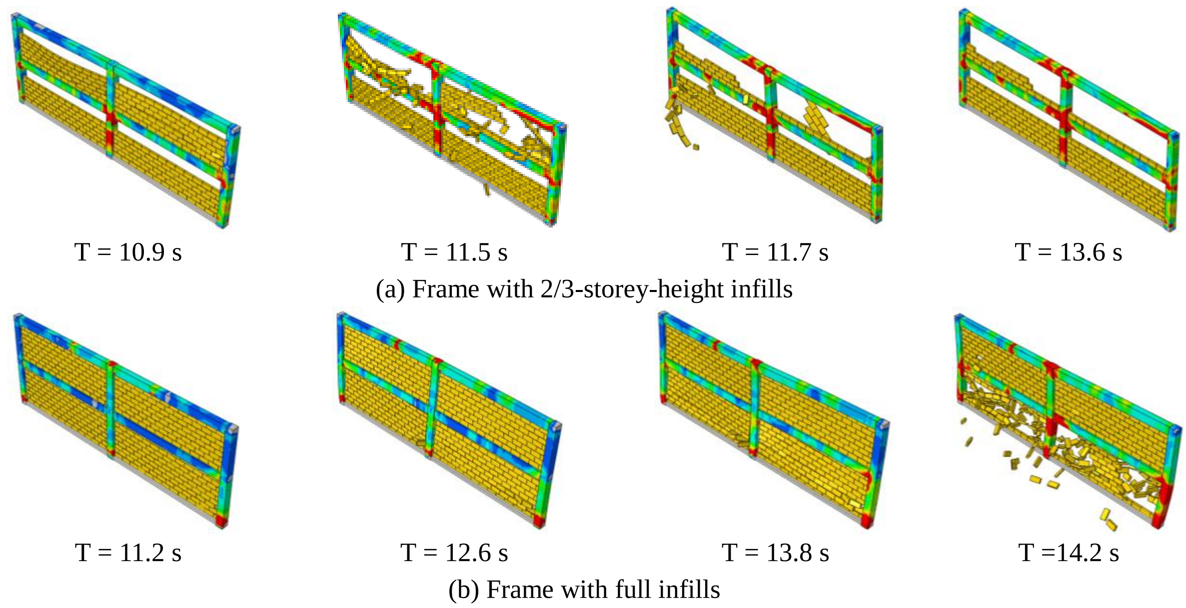

Figure 4.3. Progressive collapse of infill walls under biaxial excitation of 1999 Chi-Chi earthquake

long as the infill panels are undamaged or slightly damaged, the lateral-force transfer mechanisms of infills do not significantly influenced by out-of-plane action. However, under stronger seismic excitation, this is clearly seen in **Figure 4.1**, much severer pinching effect on the hysteresis loops occurs for the 2/3 height and fully infilled frame structures under biaxial excitation. This phenomenon is due to the out-of-plane collapse of the infill panels, as shown in **Figure 4.3**, and that leads to serious drop in the overall lateral strength and stiffness of the structures. However, the falling off of the infill panels causes different effect on the structure performance of the two infilled frame structures. As aforementioned, the fully integrated infill panels help to enhance the overall stability and vertical load-carrying capacity and therefore once they collapse, the structural stability is seriously jeopardised. The worst case is infill panels totally collapse at one particular storey, most likely the first storey, where the largest inter-storey shear takes place, since the collapse of the panels is mainly triggered by the serious damage of infills due to large in-plane diagonal forces induced by the seismic loading and then followed by disintegration of infills under the influence of out-of-plane action. When this case happens, like what is shown in **Figure 4.3**, a soft-storey, which is well known as highly vulnerable, is created and the columns in that storey would suffer serious localised damage as shown in **Figure 4.2** and this results in very poor hysteresis behaviour. On the other hand, the collapse of the infill panels in the 2/3 height infilled frame structures is likely to have some benefits on the structural performances. Under seismic excitations, short columns are created due to the deformation restraints imposed by the 2/3 height infill panels, while, on the contrast to fully integrated infill panels, they cannot provide vertical support to the structures. Therefore the damage in the frame members can lessen if the discontinuous infill panels fall off as seen in **Figure 4.2**.

5. CONCLUSION

By conducting discrete finite-element analysis with damage-based material models, the numerical simulations have successfully replicated the expected hysteresis behaviour and damage patterns of the prototype RC infilled frames under earthquakes. On the basis of the analysis results, the following conclusions are drawn. (1) The structural behaviour of infilled frame structures, unlike bare frame structures, under biaxial or uniaxial seismic excitations can be very different. (2) Under uniaxial in-plane excitations, fully integrated infill-wall panels can enhance the stability and energy dissipation of frame structures. However, under biaxial excitation, out-of-plane collapse of infills spoils the lateral-force transfer mechanisms and vertical supporting action that seriously jeopardise the structure stability. (3) The central short columns in the 2/3-storey-height infilled frame structures are experienced much severer damage due to the infill effect, as compared to the edge short columns. This is because the central columns are restrained on both sides by infills, while the edge columns are only restrained on one side, thus leading to about 1.7~2.6 times higher lateral seismic forces that are attracted by central columns under uniaxial excitation. It is also found that the damage level of frame members is reduced for the 2/3-storey-height infills, which collapse under biaxial exciations. (4) Columns of the infilled frame structures are undesirably suffered much greater damage than the adjacent connecting beam members. It reveals that the capacity design concept of “strong column-weak beam” may not be always applied to the infilled frames due to the effect of infills on the bear frame. (5) Lateral-bracing action provided by the infill panels is not significantly influenced by the out-of-plane action, provided that the infills are undamaged or just slightly damaged under low level of seismic loading.

AKCNOWLEDGEMENT

The support of Hong Kong RGC under grand No. 614011 is gratefully acknowledged.

REFERENCES

American Society of Civil Engineers (ASCE). (2006). Seismic Rehabilitation of Existing Buildings (ASCE/SEI 41), Reston, Virginia.

ABAQUS, Inc. (2010). ABAQUS Theory Manual.

Benzeggagh, M.L. and Kenanem M. (1996). Measurement of mixed-mode delamination fracture toughness of unidirectional glass/epoxy composites with mixed-mode bending apparatus. Composites Science and Technology, 56:4, 439–449.

Computers and Structures (CSI), Inc. (2010). CSI Analysis Reference Manual, Berkeley California.

Flanagan, R.D. and Bennett, R.M. (1999). Bidirectional behaviour of structural clay tile infilled frames. *Journal of Structural Engineering*, **125:3**, 236-244.

Hashemi, A. and Mosalam, K.M. (2007). Seismic evaluation of reinforced concrete buildings including effects of masonry infill walls. PEER 2007/100. UC Berkeley: PEER Center.

Kuang, J.S. and Yuen, Y.P. (2010). Effect of out-of-plane loading on in-plane behaviour of unreinforced infilled RC frames. *The International Conference on Computing in Civil and Building Engineering*, Nottingham, U.K.

Lubliner, J., Oliver, J., Oller, S. and Oñate, E. (1989). A plastic-damage model for concrete. *International Journal of Solids and Structures*, **25:3**, 229–326.

National Standard of the People’s Republic of China. (2001). Code for seismic design of buildings: GB 50011-2001, Beijing: China Architecture & Building Press.

Paulay, T. and Priestley, M.J.N. (1992). Seismic Design of Reinforced Concrete and Masonry Buildings, New York: Wiley.

Sakai, J. and Kawashima, K. (2003). Modification of the Giuffre, Menegotto and Pinto Model for unloading and reloading paths with small strain variations. *Journal of Structural Mechanics and Earthquake Engineering*, **738/I-64**, 159–169. (In Japanese)

Yuen, Y.P. and Kuang, J.S. (2011a). Seismic failure of infilled RC frames: discrete modelling approach with damage-based cohesive crack representation. *The Third International Symposium on Computational Mechanics*, Taipei, Taiwan.

Yuen, Y.P. and Kuang, J.S. (2011b). Seismic performance and vulnerabilities of infilled RC frame structures. *24th KKCNN Symposium on Civil Engineering, Hyogo, Japan*.